Correspondence to:
Professor W. Henderson,
Chemistry,
School of Science,
University of Waikato,
Private Bag 3105,
Hamilton 3240,
New Zealand
e-mail w.henderson@waikato.ac.nz

Synthesis, structural and mass spectrometric investigations of pyridinium bis(thiosalicylato)mercurate(II)

William Henderson[a,*], Jesse C. Thomas[a], Obinna C. Okpareke[a] and Edward R. T. Tiekink[b]

[a] *Chemistry, School of Science, University of Waikato, Private Bag 3105, Hamilton, New Zealand 3240*

[b] *Research Centre for Crystalline Materials, School of Science and Technology, Sunway University, 47500 Bandar Sunway, Selangor Darul Ehsan, Malaysia*

Abstract

The previously-described bis(thiosalicylato)mercury(II) complex [$Hg(SC_6H_4$-2-$CO_2H)_2$], prepared from $HgCl_2$ and thiosalicylic acid (HSC_6H_4-2-CO_2H) with added NaOH, dissolves in pyridine (py), from which the crystalline pyridinium salt $(pyH)_2[Hg(SC_6H_4$-2-$CO_2)_2]$ can be isolated as large colourless blocks. Single crystal X-ray crystallography reveals the crystal to comprise two distinct three-molecule aggregates, namely $\{Hg[SC_6H_4$-2-$C(=O)OH]_2(NC_5H_5)_2\}$ and $\{Hg[SC_6H_4$-2-$C(=O)O]_2(HNC_5H_5)_2\}$, which differ in the location of the acidic hydrogen atoms, i.e. either compound-bound for the former species or located on the pyridinium cations in the latter. The thiolate ligands are S,O-chelating and the resultant O_2S_2 four-coordinate geometries are each based on a distorted disphenoidal geometry. The three-molecule aggregates are sustained by hydroxyl-O–H···N(pyridine) hydrogen bonds in the case of $\{Hg[SC_6H_4$-2-$C(=O)OH]_2(NC_5H_5)_2\}$ whereas the second aggregate features charge-assisted pyridinium-N–H···O(carboxylate) hydrogen bonds. These aggregates are connected into a three-dimensional architecture by a combination of C–H···O, π···π, Hg···π and O···π interactions. $(pyH)_2[Hg(SC_6H_4$-2-$CO_2)_2]$ was also characterised by negative-ion ESI mass spectrometry, where it showed appreciable stability towards capillary exit voltage-induced fragmentation. In contrast, the *S*-bonded monodentate thiosalicylate complexes $RHg(SC_6H_4$-2-$CO_2)^-$ (R = Et, Ph or ferrocenyl) undergo facile decarboxylation at relatively low voltages, with the phenyl and ferrocenyl complexes subsequently forming $RHgS^-$ as an additional fragment ion at high voltages. Aggregate ions formed with the sodium counter-cations of the type $[(RHgSC_6H_4$-2-$CO_2)_nNa_{n-1}]^-$ show appreciable stability towards fragmentation.

Keywords: Mercury; Thiolate; Hydrogen bonding; Crystal structure; Electrospray ionisation mass spectrometry

1. Introduction

The thiosalicylate ligand $[SC_6H_4\text{-}2\text{-}CO_2]^{2-}$ is an interesting heterobifunctional ligand containing chemically soft thiolate and hard carboxylate donor groups. Thiosalicylate is also able to bond either as a dianion, or as a monoanion, resulting in many possible coordination modes for this ligand. As a result, the thiosalicylate ligand is able to coordinate to a diverse range of metal centres, spanning the entire Periodic Table; the coordination chemistry of this ligand has been recently reviewed.[1]

The very high affinity of mercury for thiolate ligands is well-known, and indeed the old name for thiols – *mercaptans* – reflects this high affinity.[2] Mercury is also well-known to form very stable complexes with mercaptocarboxylate ligands.[3] The long-known area of mercury thiosalicylate chemistry,[4] which has been recently summarised,[1] is exemplified by the synthesis of the bis(thiosalicylato)mercury(II) complex $[Hg(SC_6H_4\text{-}2\text{-}CO_2H)_2]$ **1** from $HgCl_2$, thiosalicylic acid and NaOH.[5] A more recent preparation omitted the use of a base.[6] $[Hg(SC_6H_4\text{-}2\text{-}CO_2H)_2]$ has been structurally characterised as its 1,4-dioxane solvate and shown to contain a linear two-coordinated mercury(II) centre; 1,4-dioxane molecules link the mercury complexes together *via* the formation of zigzag chains containing $CO_2H\cdots O(C_2H_4)_2O\cdots HO_2C$ hydrogen bonding motifs.[7] Monodentate *S*-bonded thiosalicylate ligands also coordinate to ethylmercury(II) in the well-known compound *Thiomersal*, $Na[EtHgSC_6H_4\text{-}2\text{-}CO_2]$ **2**, which has been widely employed as an anti-bacterial agent in vaccines, with some controversy.[8]

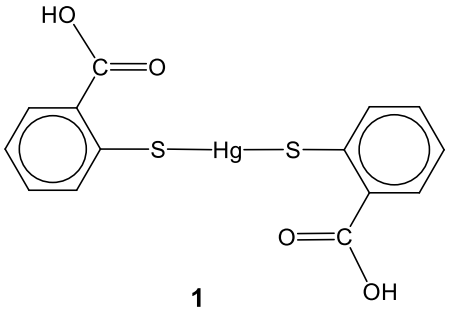

1

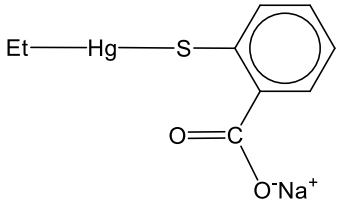

2

In mercury(II) thiosalicylate complexes the hard carboxylate O centre is also available as a secondary coordinating group, either to the same or a different metal centre, allowing the thiosalicylate ligand to act as a versatile chelating or bridging ligand. Indeed the complex [EtHgSC$_6$H$_4$-2-CO$_2$HgEt}$_2$] **3**, thought to occur as an impurity in *Thiomersal*, has been synthesised and structurally characterised.[9] The mercury(II) thiosalicylate system has been explored for its ability to act as a metalloligand through the carboxylate groups, and derivatives of [Hg(SC$_6$H$_4$-2-CO$_2$)$_2$]$^{2-}$ with a variety of metal counter-cations including Cr, Ce and Tl [10], Cu, Ag and Au [11], Pb and Cd [12] as well as group 2 and lanthanide elements [13] have been described, though none have been structurally characterised, so the coordination mode(s) remain undefined. However, [Hg(SC$_6$H$_4$-2-CO$_2$)$_2$]$^{2-}$ is able to coordinate to the Hg(PPh$_3$)$_2^{2+}$ moiety through the carboxylate oxygens to give [Hg(SC$_6$H$_4$-2-CO$_2$)$_2$Hg(PPh$_3$)$_2$] **4**, which has been structurally characterised.[14]

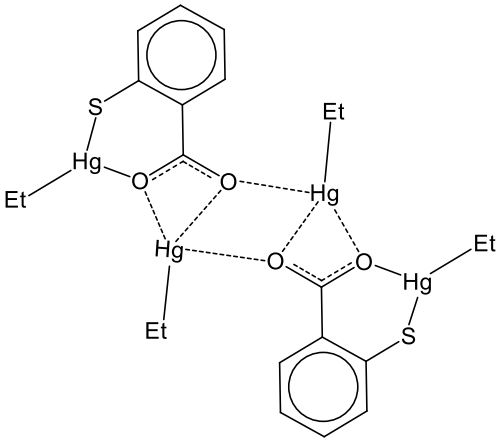

3

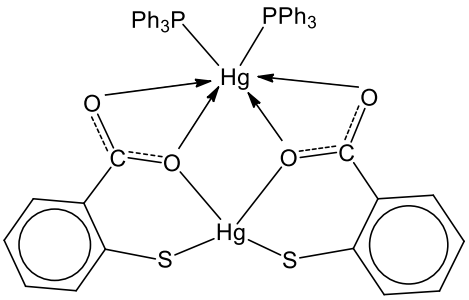

4

In view of the stability of the [Hg(SC$_6$H$_4$-2-CO$_2$)$_2$]$^{2-}$ moiety, we wished to explore the ability of [Hg(SC$_6$H$_4$-2-CO$_2$H)$_2$] to be deprotonated by suitable amine bases which would lead to the formation of salts containing the [Hg(SC$_6$H$_4$-2-CO$_2$)$_2$]$^{2-}$ anion which would then interact in the solid state with the newly formed baseH^+ cation, though the formation of hydrogen bonding interactions. The results of these investigations are described herein. We also describe

a detailed study of the ESI mass spectrometric behaviour of mercury thiosalicylate complexes, which provides insight into the coordination mode of the thiosalicylate ligand.

2. Results and discussion

2.1 Synthesis

The known bis(thiosalicylato)mercury(II) complex $[Hg(SC_6H_4\text{-}2\text{-}CO_2H)_2]$ **1** was obtained in almost quantitative yield by modification of the literature reaction [4] of mercury(II) chloride with 2 mole equivalents of each of thiosalicylic acid and base (sodium hydroxide) in water. The resulting white solid product, after filtration, washing with water and drying, was investigated as a starting material for the formation of various salts containing the $[Hg(SC_6H_4\text{-}2\text{-}CO_2)_2]^{2-}$ anion.

A portion of **1** was dissolved in pyridine, giving a pale-yellow solution and a small quantity of grey solid, presumably elemental mercury formed by decomposition. After filtration, slow evaporation of the clear solution gave large colourless blocks of **5** suitable for an X-ray diffraction study (*vide infra*). The complex is nominally formulated as $(pyH)_2[Hg(SC_6H_4\text{-}2\text{-}CO_2)_2]$, however the X-ray structure determination reveals this to be an over-simplification. Crystals of **5** lose pyridine and turn opaque when exposed to air, so no microanalytical data were obtained for this compound.

The attempted preparation of crystalline samples of other amine salts, using either ethylamine or triethylamine in conjunction with $[Hg(SC_6H_4\text{-}2\text{-}CO_2H)_2]$ was unsuccessful, giving only oils upon evaporation. Similarly, we were unable to obtain single crystals of the sodium salt, formed by dissolving $[Hg(SC_6H_4\text{-}2\text{-}CO_2H)_2]$ in the minimum amount of aqueous sodium hydroxide, and allowing the solution to slowly evaporate at room temperature. The $Ph_3PCH_2Ph^+$ salt of the $[Hg(SC_6H_4\text{-}2\text{-}CO_2)_2]^{2-}$ anion was also prepared in a one-pot procedure

by reaction of $Hg(SC_6H_4\text{-}2\text{-}CO_2H)_2$ with 2 equivalents of NaOH, and the product precipitated by addition of $[Ph_3PCH_2Ph]Cl$. Attempted crystallisation of the product by vapour diffusion of pentane into a dichloromethane solution of the colourless compound gave a mixture of crystalline and oily material.

*2.2 Description of the crystal and molecular structures of **5***

The molecular structures of the constituents of **5** are illustrated in Figs 1a and b with selected geometric parameters listed in Table 1. Based on the crystallographic analysis, the composition is formulated as $\{Hg[SC_6H_4\text{-}2\text{-}C(=O)OH]_2(NC_5H_5)_2\}\{Hg[SC_6H_4\text{-}2\text{-}C(=O)O]_2(HNC_5H_5)_2\}$, i.e. two distinct three-molecule aggregates. The difference rests with the location of the acidic hydrogen atoms. For the Hg1-containing molecule, the protons are localised on the carboxylic acid whereas for the Hg2-molecule, these are located on the pyridinium-nitrogen atoms. There is a considerable body of structural evidence to support this assignment based on geometric parameters associated with the mercury atom environments, systematic variations in the bond lengths and angles defining the carboxylic acid/carboxylate residues and in the angles subtended at the pyridyl/pyridinium nitrogen atoms.

The key difference in the immediate environments about the mercury atoms, which are based to a first approximation on a linear S–Hg–S arrangement, is seen in the magnitude of the Hg–O bonds which are systematically shorter (by up to 0.08 Å) for the Hg2 atom compared with the Hg1 atom, Table 1. Consistent with this is greater deviation of the S3–Hg2–S4 angle from linearity (by *ca* 4°). While the differences are small, systematic variations in the geometric parameters describing the carboxylic acid/carboxylate residues are evident, namely i) the more symmetric C–O bond lengths (by *ca* 0.03 Å) and ii) more symmetric O–C–C bond angles (by *ca* 2°) for the carboxylate groups in the Hg2-molecule. Finally, the angles subtended at the

protonated N3 and N4 atoms are wider (by at least 2°) than the equivalent angles for the pyridyl-nitrogen atoms.

The differences in composition notwithstanding, the overall molecular conformations in the two molecules are very similar as seen in the overlay diagram of Fig. 1c. The Hg–S bond lengths span a very narrow range, i.e. 2.3411(8) to 2.3470(8) Å, and the C–S bond lengths are experimentally equivalent (1.785(3) to 1.787(3) Å). The two bidentate chelating ligands are folded to one side of the S–Hg–S axis and give rise to a four-coordinate geometry based on a trigonal bipyramid with one equatorial site missing, i.e. a distorted disphenoidal geometry. As the result of the formation of Hg–O bonds, the carboxylic acid/carboxylate groups are twisted out of the plane of the phenyl rings to which they are connected. This is seen in the relatively narrow range of torsion angles, i.e. 35.4(4)° for C22–C23–C28–O7 to 43.1(5)° for C15–C16–C21–O5.

The three-molecule aggregate involving the Hg1-molecule is sustained by conventional hydroxyl-O–H···N(pyridine) hydrogen bonds whereas that containing the Hg2-molecule by charge-assisted pyridinium-N–H···O(carboxylate) hydrogen bonds; geometric parameters characterising these and other intermolecular interactions discussed below are given in Table 2. The most prominent feature of the molecular packing is the formation of supramolecular chains along the a-axis comprising Hg2-molecules connected on either side by pairs of pyridinium molecules linked *via* both charge-assisted pyridinium-N–H···O(carboxylate) and pyridinium-C–H···O(carboxylate) hydrogen bonds. This gives rise to non-symmetric 10-membered $\{\cdots O\cdots HNCC\}_2$ synthons, Fig. 2a. The formation of pyridinium-C–H···O(carboxylate) hydrogen bonds provides further confirmation for the presence of carboxylate groups in the Hg2-molecule. These chains are connected into a supramolecular layer parallel to $(0\ \bar{1}\ 1)$ by rows of Hg1-molecules with the links being of the type phenyl-C–H···O(hydroxyl) as well as π···π interactions between pyridine and pyridinium rings. The layer

thus formed has a flat topology, Figs 2b and c. The connections between layers are of the type Hg···π(pyridinium) and end-on O···π(pyridine, pyridinium). The importance of metal···π and element(lone-pair) contacts has been highlighted in a recent review where it was also noted that for the heavier elements these interactions can impart similar or even greater energies of stabilisation to crystals as do conventional hydrogen bonds [15].

The coordination chemistry of ligands derived from 2-mercaptobenzoic acid [1] and the isomeric 3- and 4- derivatives [16] has been reviewed very recently. In the case of mercury, coordination *via* the thiolate-sulphur atom is prevalent with the most closely related structure being that of $\{Hg[SC_6H_4\text{-}2\text{-}C(=O)OH]_2(OC_4H_8O)_2\}$, characterised as a 1:1 dioxane solvate [7]. Here, the mercury atom is linearly coordinated by two sulphur atoms and carbonyl-oxygen atoms are orientated towards the mercury centre, being separated by 3.11 Å; the hydroxyl group engages in hydrogen bonding with the dioxane-oxygen atom. A second $Hg[SC_6H_4\text{-}2\text{-}C(=O)OH]_2$ residue is known, namely in a co-crystal with $\{Hg[SC_6H_4\text{-}2\text{-}C(=O)O]_2Hg(PPh_3)_2\}$ **4**, i.e. where the carboxylate-oxygen atoms coordinate a second mercury atom [14], in a sense analogous to $\{Hg[SC_6H_4\text{-}2\text{-}C(=O)O]_2(HNC_5H_5)_2\}$ in **5** where the pyridinium groups are replaced by $(PPh_3)_2Hg$ [14]. In the molecule of $Hg[SC_6H_4\text{-}2\text{-}C(=O)OH]_2$ **1**, the coordination geometry of the mercury atom (Hg···O(carbonyl) = 2.64 and 2.68 Å) resembles the distorted disphenoidal geometries found for the mercury atoms in **5**. There are also precedents in the crystallographic literature [17] for carboxylate-O···H(ammonium) hydrogen bonding related to that seen in $\{Hg[SC_6H_4\text{-}2\text{-}C(=O)O]_2(HNC_5H_5)_2\}$ of **5**. The most closely related complex is that of *cis*-$[MoO_2(SC_6H_4\text{-}2\text{-}CO_2)_2]^{2-}$ whereby each of the pendant oxygen atoms forms a hydrogen bond with a $[HN^{(+)}Et_3]$ cation [18].

2.3 Investigation by Electrospray Ionisation Mass Spectrometry

A detailed mass spectrometric study of crystalline **5** was carried out. Crystals were poorly soluble in methanol (whereupon they turned white and opaque) and dichloromethane, but were very soluble in pyridine. A small crystal of the compound was dissolved in a few drops of pyridine, and diluted with methanol for mass spectrometric analysis in negative-ion mode. The observed ions are summarised in Table 3. The same ions, in approximately the same relative intensities, were observed when a crystal of **5** was analysed in methanol alone (without prior dissolution in pyridine). Identification of mercury-containing ions is readily facilitated by the distinctive isotopic signature of mercury, which has seven naturally-occurring isotopes.

At moderate capillary exit voltages (e.g. 120 V), the *pseudo*-parent ion $[Hg(SC_6H_4\text{-}2\text{-}CO_2)_2 + H]^-$ was observed as the base peak at *m/z* 506.99 (calculated 506.96), together with two lower intensity ions due to $[Hg_2(SC_6H_4\text{-}2\text{-}CO_2)_3 + H]^-$ at *m/z* 858.97 (calculated 858.93) and $[Hg_2(SC_6H_4\text{-}2\text{-}CO_2)_4 + 3H]^-$ (*m/z* 1012.99, calculated 1012.94), as shown in Fig. 3. The dianionic species $[Hg(SC_6H_4\text{-}2\text{-}CO_2)_2]^{2-}$ was not observed in the mass spectrum. Increasing the capillary exit voltage to 150 V resulted in a decrease in the intensity of the *m/z* 1012.99 ion, whereas decreasing the capillary exit voltage to 60 V resulted in this ion becoming the base peak, with $[Hg(SC_6H_4\text{-}2\text{-}CO_2)_2 + H]^-$ (*m/z* 506.99) and a new ion assigned as $[Hg(SC_6H_4\text{-}2\text{-}CO_2H)_3]^-$ at *m/z* 660.99 (calculated 660.97) at lower relative intensity. This latter ion is of low intensity (*ca* 10%) at 90 V, and is not observed at 120 V. Additionally, a low intensity ion observed at 60 V is the chloride adduct $[Hg(SC_6H_4\text{-}2\text{-}CO_2H)_2 + Cl]^-$ at *m/z* 542.96 (calculated *m/z* 542.94). The presence of the two chlorine isotopes (^{35}Cl 75.8%, ^{37}Cl 24.2%) has a distinct influence on the isotope pattern of this ion, when compared to (non-chlorine containing) $[Hg(SC_6H_4\text{-}2\text{-}CO_2)_2 + H]^-$ at *m/z* 506.99. The source of chloride in $[Hg(SC_6H_4\text{-}2\text{-}CO_2H)_2 + Cl]^-$ is presumably from the use of $HgCl_2$ as a starting material. It is noteworthy that no pyridinium

adduct ions were observed in the mass spectrum, with all charge diminution being achieved by protonation.

When a sample of **5** was analysed in pyridine-methanol solution with added NaCl, at a capillary exit voltage of 120 V, $[Hg(SC_6H_4\text{-}2\text{-}CO_2)_2 + H]^-$ (*m/z* 506.99) remained the base peak, but the intensity of $[Hg(SC_6H_4\text{-}2\text{-}CO_2H)_2 + Cl]^-$ (*m/z* 542.96) decreased, and was replaced by two new ions, $[Hg(SC_6H_4\text{-}2\text{-}CO_2H)Cl]^-$ at *m/z* 388.91 and $[Hg(SC_6H_4\text{-}2\text{-}CO_2)_2 + Na]^-$ at *m/z* 528.92.

The benzyltriphenylphosphonium salt, $(Ph_3PBz)_2[Hg(SC_6H_4\text{-}2\text{-}CO_2)_2]$, was also analysed by negative ion ESI MS in acetonitrile-methanol solution, where it showed $[Hg(SC_6H_4\text{-}2\text{-}CO_2)_2 + H]^-$ at *m/z* 506.99 as the base peak, but now (in contrast to the pyridinium salt) with the dianion $[Hg(SC_6H_4\text{-}2\text{-}CO_2)_2]^{2-}$ observed at *m/z* 252.95, the latter ion having the characteristic 0.5 *m/z* separation of adjacent peaks in its isotope pattern.

Following the observation of chloride-containing ions it was of interest to characterise the known compound $[Hg(SC_6H_4\text{-}2\text{-}CO_2H)_2]$ **1** [5] itself, since its preparation utilises a chloride source ($HgCl_2$). The ion $[Hg(SC_6H_4\text{-}2\text{-}CO_2)_2 + H]^-$ (*m/z* 506.99) was the base peak in the spectrum at 120 V, together with $[Hg(SC_6H_4\text{-}2\text{-}CO_2H)Cl]^-$ (*m/z* 388.91, 26%), $[Hg(SC_6H_4\text{-}2\text{-}CO_2)_2 + Na]^-$ (*m/z* 528.92, 20%), along with a number of low-intensity, higher mass ions which include $[Hg_2(SC_6H_4\text{-}2\text{-}CO_2)_3 + H]^-$ (*m/z* 858.93), and the series $[Hg_2(SC_6H_4\text{-}2\text{-}CO_2)_4 + xNa + (3\text{-}x)H]^-$ (x = 0, *m/z* 1012.95; x = 1, *m/z* 1034.93; x = 2, *m/z* 1056.92; x = 3, *m/z* 1077.90). Interestingly, at a low capillary exit voltage (60 V), the base peak was $[Hg(SC_6H_4\text{-}2\text{-}CO_2H)_2 + Cl]^-$ (*m/z* 542.96) which was only observed as a low intensity ion in crystalline $(pyH)_2[Hg(SC_6H_4\text{-}2\text{-}CO_2)_2]$, presumably because this sample is freed of the majority of chloride ions during the crystallisation of the complex from pyridine.

When the negative-ion ESI mass spectra of either $(pyH)_2[Hg(SC_6H_4\text{-}2\text{-}CO_2)_2]$ **5** or $[Hg(SC_6H_4\text{-}2\text{-}CO_2H)_2]$ **1** were recorded at elevated capillary exit voltages (> 150 V), there was no evidence of decarboxylation occurring. This is similar behaviour to that shown by other complexes containing chelating thiosalicylate dianion ligands, such as complexes of platinum(II) [19] and gold(III) [20], but is in marked contrast to the mass spectrometric behaviour of *Thiomersal*, $[EtHgSC_6H_4\text{-}2\text{-}CO_2]^-$ (*vide infra*). This complex contains an *S*-bonded, monodentate thiosalicylate ligand, and undergoes facile decarboxylation at relatively low capillary exit voltages. Although there have been a number of mass spectrometric investigations of the interactions of *Thiomersal* with molecules of biological relevance, such as haemoglobin,[21] proteins (human serum albumin and β-lactoglobulin A) [22], glutathione [23,24], cysteine [24] and DNA [24] the ESI mass spectrometric behaviour of *Thiomersal* itself does not appear to have been investigated to date.

The negative-ion ESI mass spectrum of $Na[EtHgSC_6H_4\text{-}2\text{-}CO_2]$ in methanol at a low capillary exit voltage (60 V) showed, in the low mass range (< *m/z* 1000), $[EtHgSC_6H_4\text{-}2\text{-}CO_2]^-$ as the base peak at *m/z* 383.03 (calculated 383.00). A capillary exit voltage of 80 V marks the onset of decarboxylation, shown by the ion $[EtHgSC_6H_4]^-$ at *m/z* 339.02 (calculated 339.01). At 120 V, this ion is the base peak, with $[EtHgSC_6H_4\text{-}2\text{-}CO_2]^-$ at *ca* 60% relative intensity. An illustrative spectrum at a capillary exit voltage of 150 V is shown in Fig. 4. The ion at *m/z* 787.11 is assigned to the aggregate ion $[(EtHgSC_6H_4\text{-}2\text{-}CO_2)_2Na]^-$ (calculated *m/z* 786.99), however it is interesting that there are no corresponding dimercury ions that are decarboxylated, suggesting that the interaction with the sodium ion reduces the propensity for decarboxylation. This is further illustrated by the wide *m/z* range negative ion spectrum at a capillary exit voltage of 150 V (Fig. 5) which shows a series of aggregate ions of the type $[(EtHgSC_6H_4\text{-}2\text{-}CO_2)_nNa_{n-1}]^-$, with the n = 2 ion the base peak. Such aggregation behaviour is typical of sodium salts in ESI MS, for example sodium formate [25] which is often used as a mass calibrant over a wide

range of *m/z* values. Although the parent ion (n = 1) $[EtHgSC_6H_4\text{-}2\text{-}CO_2]^-$ shows considerably less decarboxylation under these conditions, the aggregate ions do not show any significant decarboxylated counterparts. Addition of a small amount of trifluoroacetic acid (4 drops 0.01% aqueous solution) to the *Thiomersal* analyte solution did not change the appearance of the spectrum, indicating the preference for aggregation with the sodium ion.

Somewhat surprisingly, *Thiomersal* shows ions stable to very high capillary exit voltages in its positive-ion ESI mass spectra. For example, at 330 V (the highest capillary exit voltage possible on the MicrOTOF mass spectrometer used), the mercury-containing ions $[(EtHgSC_6H_4\text{-}2\text{-}CO_2)_nNa_{n+1}]^+$ with n = 1 (*m/z* 428.97, calculated 428.98), n = 2 (*m/z* 832.98, calculated 832.97) and n = 3 (*m/z* 1236.96, calculated 1236.96) were observed as the three most intense peaks in the spectrum, with no associated decarboxylated ions.

The behaviour of *Thiomersal* with added thiosalicylic acid is readily explored by ESI MS, and provides some interesting observations. At a low capillary exit voltage (60 V), in addition to the expected ion $[EtHgSC_6H_4\text{-}2\text{-}CO_2]^-$ (*m/z* 382.99), a protonated aggregate ion $[(EtHgSC_6H_4\text{-}2\text{-}CO_2)_2H]^-$ was observed at *m/z* 765.00. This is in contrast to *Thiomersal* itself, which shows the sodiated ion $[(EtHgSC_6H_4\text{-}2\text{-}CO_2)_2Na]^-$ (calculated *m/z* 786.99). In addition, ions due to the free thiosalicylate anion $[HSC_6H_4\text{-}2\text{-}CO_2H - H]^-$ (*m/z* 153.00), and the adduct $[EtHgSC_6H_4\text{-}2\text{-}CO_2\cdot HSC_6H_4\text{-}2\text{-}CO_2H]^-$ (*m/z* 537.00) were also observed. Although the structure of this latter ion cannot be inferred from mass spectrometry alone, organomercury(II) compounds have a strong tendency to retain two coordination, as shown by the paucity of X-ray structures of compounds where an organomercury centre is coordinated to two (or more) sulphur donor ligands.[26,27,28,29] It may be a hydrogen-bonded adduct between the carboxylate anion of the *Thiomersal*, with the carboxylic acid group of free thiosalicylic acid. This adduct is, in any event, very weakly associated, since it is not observed at the slightly higher capillary exit voltage of 90 V. Another new ion of interest in the mass spectrum is the

observation of the dealkylated species $[Hg(SC_6H_4\text{-}2\text{-}CO_2H)_3]^-$ at *m/z* 660.96. Wu *et al*. [24] have previously investigated the thiol exchange reactions of *Thiomersal* towards added thiols, which liberate thiosalicylic acid, but they did not observe dealkylation of the mercury.

A selection of other closely-related organomercury(II) thiosalicylate complexes were prepared for comparative purposes with *Thiomersal*, in order to confirm the generality of decarboxylation in this type of complex. Thus, reactions of RHgCl (R = Ph or ferrocenyl, Fc) with one mole equivalent of thiosalicylic acid and 2 equiv. of NaOH in methanol gave the thiosalicylate complexes $Na[RHgSC_6H_4\text{-}2\text{-}CO_2]$ as white or orange powders, respectively. The phenyl compound has been known for some time,[30] including its free acid $PhHgSC_6H_4\text{-}2\text{-}CO_2H$,[31,32] but the ferrocenyl compound has not been reported previously. The compounds $Na[RHgSC_6H_4\text{-}2\text{-}CO_2]$ (R = Ph, Fc) show analogous behaviour to *Thiomersal* at relatively low capillary exit voltages, with the parent $[RHgSC_6H_4\text{-}2\text{-}CO_2]^-$ undergoing facile decarboxylation to $[RHgSC_6H_4]^-$, though there was a difference in the tendency for decarboxylation to occur for the two compounds. Thus at a capillary exit voltage of 100 V, $Na[PhHgSC_6H_4\text{-}2\text{-}CO_2]$ shows $[PhHgSC_6H_4\text{-}2\text{-}CO_2]^-$ (*m/z* 430.96, calculated 431.00) and $[PhHgSC_6H_4]^-$ (*m/z* 386.97, calculated 387.01) with relative intensities of 100 and 30% respectively, but for $Na[FcHgSC_6H_4\text{-}2\text{-}CO_2]$ only the parent ion $[FcHgSC_6H_4\text{-}2\text{-}CO_2]^-$ (*m/z* 538.93, calculated 538.97) was observed, with no indication of decarboxylation at this voltage. At 150 V, the relative intensities for $Na[PhHgSC_6H_4\text{-}2\text{-}CO_2]$ were $[PhHgSC_6H_4\text{-}2\text{-}CO_2]^-$ (12%) and $[PhHgSC_6H_4]^-$ (100%), indicating substantial decarboxylation (Fig. 6), but for $Na[FcHgSC_6H_4\text{-}2\text{-}CO_2]$ the relative intensities were $[FcHgSC_6H_4\text{-}2\text{-}CO_2]^-$ (100%) and $[FcHgSC_6H_4]^-$ (*m/z* 494.94, calculated 494.98, 58%). These observations indicate that $[PhHgSC_6H_4\text{-}2\text{-}CO_2]^-$ undergoes decarboxylation more readily when compared to the ferrocenyl analogue. However, as observed for $[EtHgSC_6H_4\text{-}2\text{-}CO_2]^-$, the examination of $Na[PhHgSC_6H_4\text{-}2\text{-}CO_2]$ at higher capillary exit voltages (150-180 V) across a wide *m/z* range indicates that under conditions

where the parent ion $[PhHgSC_6H_4\text{-}2\text{-}CO_2]^-$ undergoes extensive fragmentation the aggregate ions $[(PhHgSC_6H_4\text{-}2\text{-}CO_2)_2Na]^-$ (*m/z* 883) and $[(PhHgSC_6H_4\text{-}2\text{-}CO_2)_3Na_2]^-$ (*m/z* 1335) show no associated fragments.

Another feature in the mass spectra of $[RHgSC_6H_4\text{-}2\text{-}CO_2]^-$ (R = Ph or Fc) is the observation of the ions $[RHgS]^-$ (R = Ph, *m/z* 310.93, calculated 310.98; R = Fc, *m/z* 418.91, calculated 418.95) at elevated capillary exit voltages (illustrated in Fig. 6 for the Ph system). This ion was more readily formed in the phenyl system, with $[PhHgS]^-$ having 92% relative intensity compared to the base peak of $[PhHgSC_6H_4]^-$ (*m/z* 386.97, 100%) at a capillary exit voltage of 180 V. At this voltage, the corresponding $[FcHgS]^-$ ion had very low intensity (*ca* 1%), but increased above 180 V. The corresponding $[EtHgS]^-$ ion was not observed in spectra of *Thiomersal* at high capillary exit voltages. It is possible that the phenyl ring provides resonance stabilisation of the negative charge, stabilising the $PhHgS^-$ ion. This species is conceptually related to the known mercaptan complex PhHgSH,[33] by deprotonation.

Decarboxylation of carboxylate anions has been known for some time,[34,35] and decarboxylation is also well-known to occur in metal carboxylate complex ions,[36,37] in complexes of amino acids or peptides [38], and complexes of carboxylate-containing carbohydrates.[39] The results of these mass spectrometry investigations indicates that the coordination of the carboxylate group of the thiosalicylate ligand to mercury provides significant protection against capillary exit voltage-induced decarboxylation. The stability of organomercury thiosalicylate aggregate ions with the Na^+ counterion also affords similar protection.

3. Conclusions

The pyridinium salt of the bis(thiosalicylate)mercurate(II) ion, **5**, has been synthesised

by a simple procedure. Crystallography shows **5** to comprise two distinct three-molecule aggregates and formulated as $\{Hg[SC_6H_4\text{-}2\text{-}C(=O)OH]_2(NC_5H_5)_2\}\{Hg[SC_6H_4\text{-}2\text{-}C(=O)O]_2(HNC_5H_5)_2\}$. The key difference between the aggregates relates to the positioning of the acidic hydrogen atoms, which are on the oxygen atoms in the former and on the pyridinium cations in the latter. The O_2S_2 atoms derived from the chelating thiolate ligands define a distorted disphenoidal geometry.

A detailed study of **5** and a selection of other mercury thiosalicylate complexes using ESI MS provides correlations with the carboxylate coordination mode, and identifies the role of coordination in providing stabilisation through the formation of aggregate ions. We are currently exploring the mass spectrometric behaviour of other organomercury mercaptocarboxylates and results will be reported in due course.

4. Experimental

4.1 Instrumentation

ESI mass spectra were recorded on Bruker MicrOTOF mass spectrometer that was periodically calibrated using methanolic sodium formate. Typical parameters used a *Capillary Exit* voltage of 150 V and a *Skimmer 1* voltage of 50 V, though these parameters were varied to explore aggregation and/or fragmentation processes (maintaining a *Capillary Exit* : *Skimmer 1* ratio of 3:1). Assignment of ions employed a comparison of experimental and theoretical isotope patterns, the latter calculated using instrument-based software, or the open-source software *mMass*.[40] Reported *m/z* values are for the most intense isotopomer in the isotope distribution pattern.

4.2 Materials

Thiosalicylic acid (Sigma), mercury(II) chloride (BDH), phenylmercuric chloride (BDH), *Thiomersal* (BDH) and pyridine (BDH) were used as supplied; other chemicals were at least of reagent grade and were used as supplied. The compounds FcHgCl [41] and (Ph_3PBz)Cl [42] were prepared by the literature procedure.

4.3 Synthesis of $Hg(SC_6H_4\text{-}2\text{-}CO_2H)_2$ ***1***

This compound was prepared by a modification of the literature procedure.[5] To a suspension of thiosalicylic acid (2.745 g, 17.8 mmol) in water (30 mL) was added sodium hydroxide (0.734 g, 18.4 mmol) and the mixture briefly stirred to give a pale-yellow solution. This solution was then added to a stirred solution of mercury(II) chloride (2.42 g, 8.9 mmol) in distilled water (50 mL) resulting in the immediate formation of a white precipitate. The mixture was stirred at room temperature for 3 h and the white solid product was filtered, washed with distilled water (2 x 20 mL), and dried under vacuum to give the product (4.439 g, 98%). The compound was characterised using negative-ion ESI MS (refer text).

4.4 Synthesis of the pyridinium salt $(pyH)_2[Hg(SC_6H_4\text{-}2\text{-}CO_2)_2]$ ***5***

Approximately 0.5 g of crude $Hg(SC_6H_4\text{-}2\text{-}CO_2H)_2$ was dissolved in pyridine (5 mL) in a glass vial to give a pale-yellow solution, with a small amount of insoluble grey matter (presumably elemental mercury). The solution was filtered to give a clear-yellow solution which was then allowed to spontaneously evaporate at room temperature. When solid started to form, the vial was sealed and the solution allowed to stand at room temperature for several

weeks to give a number of large, clear and colourless block crystals, that were structurally characterised (see Sections 2.2 and 4.9). ESI MS data are summarised in Table 1.

4.5 Synthesis of $(Ph_3PBz)_2[Hg(SC_6H_4\text{-}2\text{-}CO_2)_2]$

$HgCl_2$ (1.21 g, 4.46 mmol) and thiosalicylic acid (1.37 g, 8.90 mmol) were suspended in 50 mL water. A solution of sodium hydroxide (0.734 g, 18.3 mmol) in water (20 mL) was added dropwise with stirring, to give a slightly cloudy, grey solution, which was stirred for 1 h. The solution was filtered to give a clear pale-yellow solution. To this solution was then added dropwise with stirring a solution of $(Ph_3PBz)Cl$ (3.77 g, 9.70 mmol) in water (30 mL), which quickly deposited a light-brown oil. At the end of the addition, on continued stirring the oil solidified to a white solid. The lumps of solid were manually broken up, the solid filtered, washed with water (2 x 20 mL) and dried under vacuum to give the crude product (4.717 g). Recrystallisation of a sample by vapour diffusion of pentane into a dichloromethane solution gave some oily sticky crystals, which were washed with isopropanol (0.5 mL). A crystal was removed for ESI MS analysis in MeCN/MeOH solution.

4.6 Synthesis of $Na[PhHgSC_6H_4\text{-}2\text{-}CO_2]$

PhHgCl (2.00 g, 6.39 mmol) was suspended in methanol (20 mL), and to the stirred suspension was added sequentially thiosalicylic acid (0.986 g, 6.40 mmol) followed by dropwise addition of a solution of sodium hydroxide (0.52 g, 12.97 mmol) in methanol (20 mL). The mixture was briefly warmed to *ca* 50 ℃ to give a slightly cloudy pale-yellow solution, containing some dark suspended matter (presumably elemental mercury). The solution was filtered through glass fibre filter paper, and the filtrate evaporated to dryness to give an off-white solid. Water (10 mL) was added and the resulting white solid triturated to dissolve

sodium chloride by-product. After allowing the mixture to partly evaporate for 24 h, the product was filtered, washed with 2 mL cold water, and dried under vacuum to give 0.832 g (29 %) of white solid. Found: C 34.31, H 2.28. $C_{13}H_9HgNaO_2S$ requires C 34.47, H 2.00%.

4.7 Synthesis of Na[FcHgSC$_6$H$_4$-2-CO$_2$]

A solution of sodium hydroxide (0.1937 g, 4.83 mmol) in methanol (10 mL) was added to a solution of thiosalicylic acid (0.3736 g, 2.43 mmol) in methanol (30 mL) with stirring. To the resulting stirred solution was added FcHgCl (1.0188 g, 2.42 mmol), resulting in the formation of a bright-orange precipitate and an orange supernatant. The product was filtered, washed with a small volume of methanol and then water to remove soluble salts, and dried under vacuum to give the product as a bright-orange solid (0.56 g, 41%). Satisfactory microanalytical data could not be obtained for this sample, either the initially isolated solid, or a sample recrystallised by dissolving in the minimum amount of warm DMF, followed by cooling to room temperature, giving fine, bright-orange needles. The identity of the sample is therefore based on its mass spectral characterisation.

4.8 Reactivity of Na[EtHgSC$_6$H$_4$-2-CO$_2$] (Thiomersal) towards thiosalicylic acid

Equimolar amounts of *Thiomersal* (96.6 mg) and thiosalicylic acid (37 mg) were dissolved in methanol (10 mL), and the mass spectrum recorded after 30 min.

4.9 Single crystal X-ray structure determination of (pyH)$_2$[Hg(SC$_6$H$_4$-2-CO$_2$)$_2$] ***5***

Crystals of **5** were obtained from [Hg(SC$_6$H$_4$-2-CO$_2$H)$_2$] **1** in pyridine as described in Section 4.4. Intensity data were measured for a colourless crystal (0.02 × 0.04 × 0.10 mm) at

100 K on an Rigaku/Oxford Diffraction XtaLAB Synergy diffractometer (Dualflex, AtlasS2) fitted with CuKα radiation (λ = 1.54178 Å) so that θ_{max} = 67.1°. Data reduction and Gaussian absorption corrections were by standard methods [43]. The structure was solved by direct methods [44] and refined on F^2 [45] with anisotropic displacement parameters and C-bound H atoms included in the riding model approximation. The O- and N-bound H atoms were refined with distance constraints 0.84±0.01 and 0.88±0.01 Å, respectively. A weighting scheme of the form $w = 1/[\sigma^2(F_o^2) + (0.031P)^2 + 1.848P]$ where $P = (F_o^2 + 2F_c^2)/3$) was introduced. Three reflections, i.e. (8 3 1), (6 1 5) and (-8 3 1), were omitted from the final cycles of refinement owing to poor agreement. The maximum and minimum residual electron density peaks of 1.62 and 0.87 eÅ^{-3} were located, respectively, 1.04 and 0.79 Å from the Hg1 atom. The molecular structure diagrams showing 70% probability displacement ellipsoids were generated by ORTEP for Windows [46], the overlay diagram with QMol [47] and the packing diagrams with DIAMOND [48]. Additional data analysis was made with PLATON [49].

Crystal data for 5: $C_{48}H_{40}Hg_2N_4O_8S_4$, M = 1330.26, triclinic, $P\bar{1}$, a = 9.93980(10), b = 15.6039(2), c = 17.5606(3) Å, α = 116.369(2), β = 90.5790(10), γ = 105.2420(10)°, V = 2328.92(7) Å^3, Z = 2, D_x = 1.897 g cm^{-3}, F(000) = 1288, μ = 13.821 mm^{-1}, no. reflns meas. = 54839, no. unique reflns = 8300 (R_{int} = 0.041), no. reflns with $I \geq 2\sigma(I)$ = 7733, no. parameters = 607, R(obs. data) = 0.021, $wR2$(all data) = 0.054. CCDC deposition number: 1889486.

Notes

The authors declare that they have no conflicts of interest with the contents of this article.

Acknowledgements

We thank the University of Waikato for supporting the synthesis and mass spectrometric measurements. The Research Centre for Crystalline Materials (Sunway University) is thanked for the X-ray intensity data.

Supplementary materials

Crystallographic data for compound **5** reported in this paper have been deposited with the Cambridge Crystallographic Data Centre (CCDC) as supplementary publication no. CCDC-1889486. These data can be obtained free of charge via www.ccdc.cam.ac.uk/getstructures.

Table 1 Geometric parameters (Å, °) for the molecular structure of **5**.

Hg1–S1	2.3411(8)	Hg2–S3	2.3443(8)
Hg1–S2	2.3460(8)	Hg2–S4	2.3470(8)
Hg1–O1	2.580(2)	Hg2–O5	2.498(2)
Hg1–O3	2.563(2)	Hg2–O7	2.499(2)
C–S1, S2	1.785(3), 1.786(3)	C–S3, S4	1.786(3), 1.787(3)
C7–O1, O2	1.234(4), 1.299(4)	C21–O5, O6	1.237(4), 1.285(4)
C14–O3, O4	1.227(4), 1.310(4)	C28–O7, O8	1.240(4), 1.276(4)
S1–Hg1–S2	173.04(3)	S3–Hg1–S4	169.03(3)
S1–Hg1–O1	81.67(5)	S3–Hg1–O5	84.08(6)
S1–Hg1–O3	104.11(5)	S3–Hg1–O7	106.55(6)
S2–Hg1–O1	103.57(5)	S4–Hg1–O5	104.51(6)
S2–Hg1–O3	81.78(5)	S4–Hg1–O7	82.26(6)
O1–Hg1–O3	76.11(7)	O5–Hg1–O7	77.87(9)
Hg1–S1–C1	100.36(10)	Hg2–S3–C15	100.76(10)
Hg1–S2–C8	98.51(10)	Hg2–S4–C22	100.34(10)
Hg1–O1–C7	122.71(19)	Hg2–O5–C21	124.35(19)
Hg1–O3–C14	121.2(2)	Hg2–O7–C28	125.7(2)
O1–C7–O2	122.9(3)	O5–C21–O6	122.9(3)
O1–C7–C2	123.6(3)	O5–C21–C16	122.5(3)
O2–C7–C2	113.5(2)	O6–C21–C16	114.6(3)
O3–C14–O2	122.4(3)	O7–C28–O6	122.9(3)
O3–C14–C9	124.4(3)	O7–C28–C23	122.2(3)
O4–C14–C9	113.1(3)	O8–C28–C23	114.8(3)
C29–N1–C33	118.7(3)	C39–N3–C43	121.1(3)
C34–N2–C38	118.3(3)	C44–N4–C48	120.9(3)

Table 2 Geometric parameters (Å, °) characterising the intermolecular interactions in the crystal of **5**.[a]

A	H	D	H…D	A…D	A-H…D	Symmetry operation
O2	H2o	N1	1.70(4)	2.549(4)	178(4)	x, y, z
O4	H4o	N2	1.76(4)	2.600(4)	171(4)	x, y, z
N3	H3n	O6	1.67(2)	2.556(4)	176(4)	x, y, z
N4	H4n	O8	1.66(3)	2.542(4)	177(4)	x, y, z
C43	H43	O8	2.30	3.242(4)	172	-1+x, y, z
C48	H48	O6	2.28	3.213(4)	165	1+x, y, z
C27	H27	O2	2.52	3.353(4)	146	x, y, z
Cg(1)	–	Cg(2)	–	3.6889(19)	11.16(16)[b]	x, y, z
Cg(3)	–	Cg(4)	–	3.589(2)	4.00(19)[b]	-1+x, -1+y, -1+z
C28	O8	Cg(3)	3.496(3)	4.734(4)	163.6(2)	1-x, 1-y, 2-z
C14	O4	Cg(1)	3.253(3)	4.438(4)	150.0(2)	-x, 1-y, 1-z

[a] Cg(1)-Cg(4) are the ring centroids of the (N1,C29-C33), (N3,C39-C43), (N2,C34-38) and (N4,C44-C48) rings, respectively.

[b] The specified angle is the angle of inclination between the rings.

Table 3 Ions observed in the negative-ion ESI mass spectra of **5** in pyridine-methanol solution at a range of capillary exit voltages.

Ions	*m/z*	Approx. intensity at capillary exit voltage (V)			
		60	**90**	**120**	**150**
$[Hg(SC_6H_4\text{-}2\text{-}CO_2)_2 + H]^-$	506.98	50	100	100	100
$[Hg(SC_6H_4\text{-}2\text{-}CO_2H)_2 + Cl]^-$	542.96	4	2	-	-
$[Hg(SC_6H_4\text{-}2\text{-}CO_2H)_3]^-$	660.99	46	12	-	1
$[Hg_2(SC_6H_4\text{-}2\text{-}CO_2)_3 + H]^-$	858.97	-	3	7	26
$[Hg_2(SC_6H_4\text{-}2\text{-}CO_2)_4 + 3H]^-$	1012.99	100	54	10	5

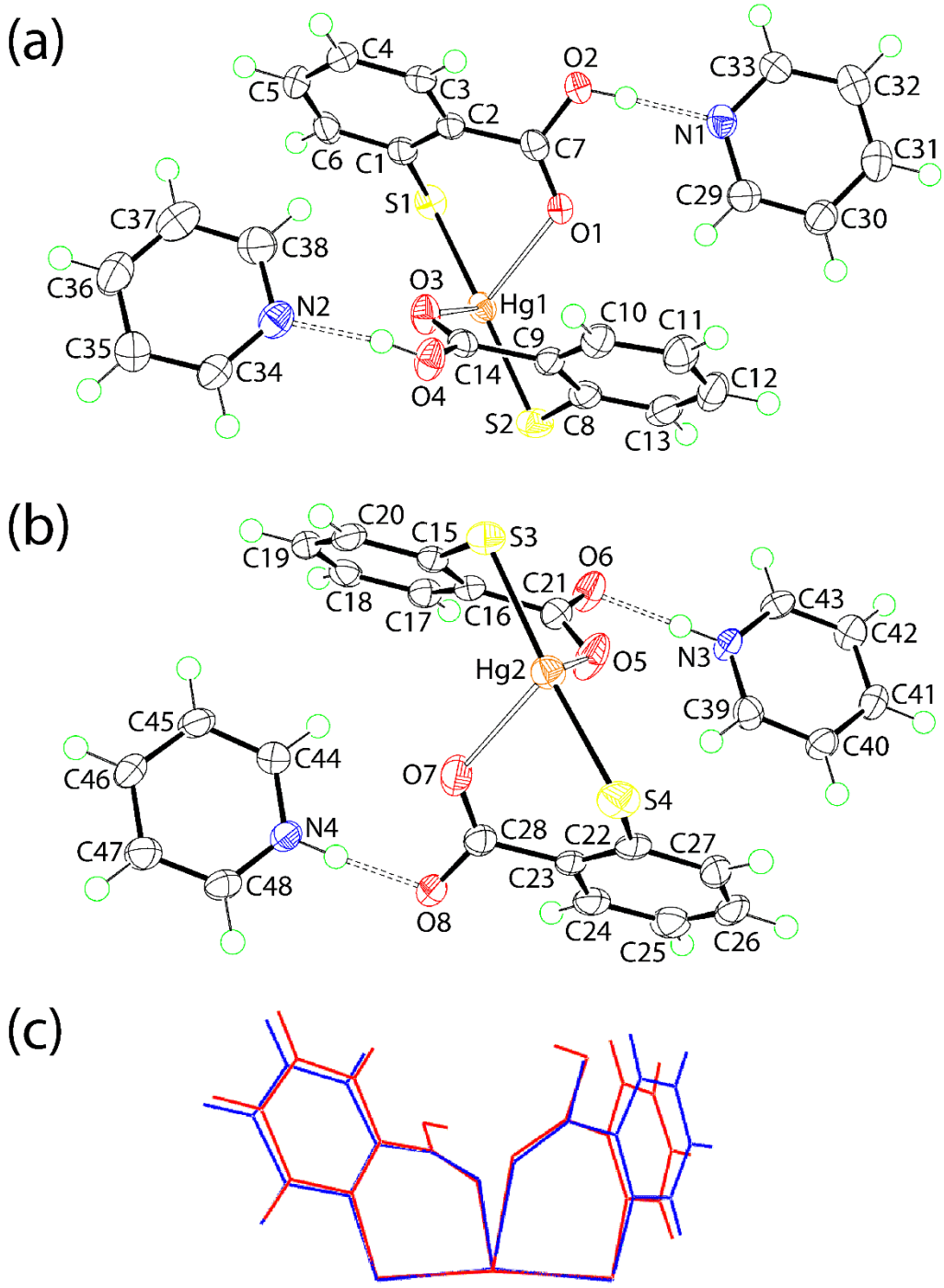

Fig. 1. Molecular structures of the constituents of **5**, showing atom labelling schemes and displacement ellipsoids at the 70% probability level: (a) $\{Hg[SC_6H_4\text{-}2\text{-}C(=O)OH]_2(NC_5H_5)_2\}$ and (b) $\{Hg[SC_6H_4\text{-}2\text{-}C(=O)O]_2(HNC_5H_5)_2\}$. (c) Overlay diagram of the Hg1- (red image) and (inverted) Hg2-containing (blue) molecules. The molecules have been overlapped so that the S–Hg–S atoms are coincident.

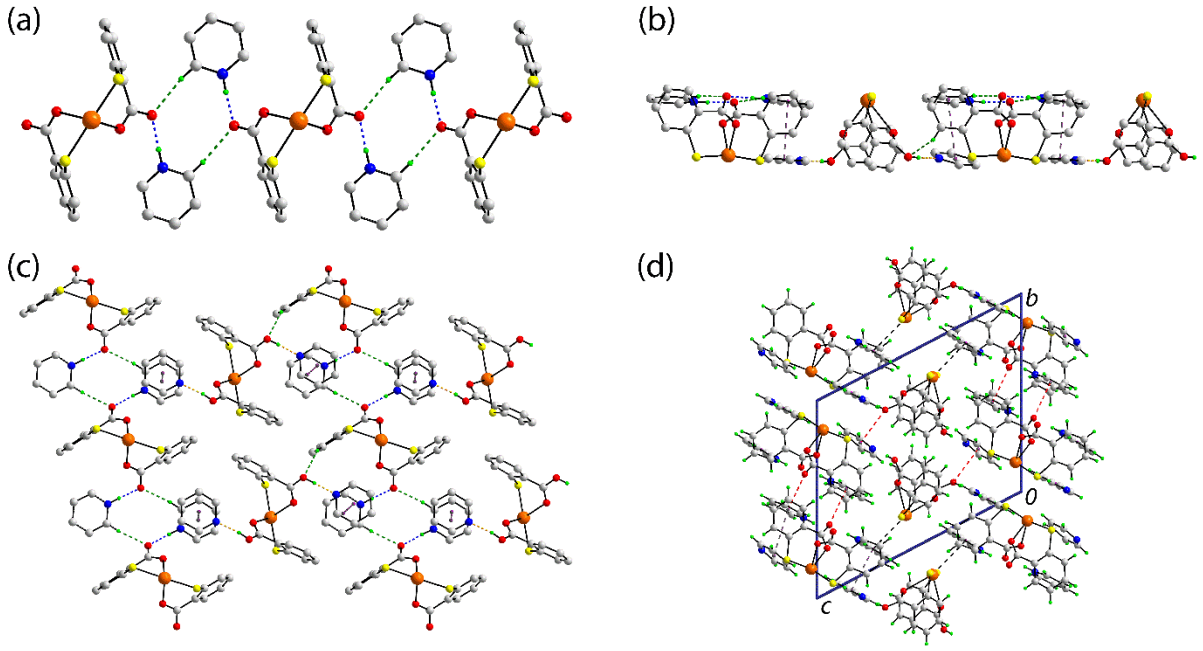

Fig. 2. Supramolecular association in the crystal of **5**: (a) a view of the supramolecular chain comprising Hg2-molecules linked by charge-assisted pyridinium-N–H···O(carboxylate) and pyridinium-C–H···O(carboxylate) hydrogen bonds shown as blue and green dashed lines, respectively, (b) side-on and (c) plan views of the supramolecular layers approximately parallel to (0 $\bar{1}$ 1). The hydroxyl-O–H···N(pyridine) hydrogen bonds and π···π interactions are shown as orange and purple dashed lines, respectively. In (a)-(c), non-participating hydrogen atoms have been omitted for reasons of clarity. (d) A view of the unit cell contents shown in projection down the a-axis. The Hg···π(pyridinium) and O···π(pyridine, pyridinium) interactions are shown as black and red dashed lines, respectively. For clarity, the intra-layer contacts are not indicated.

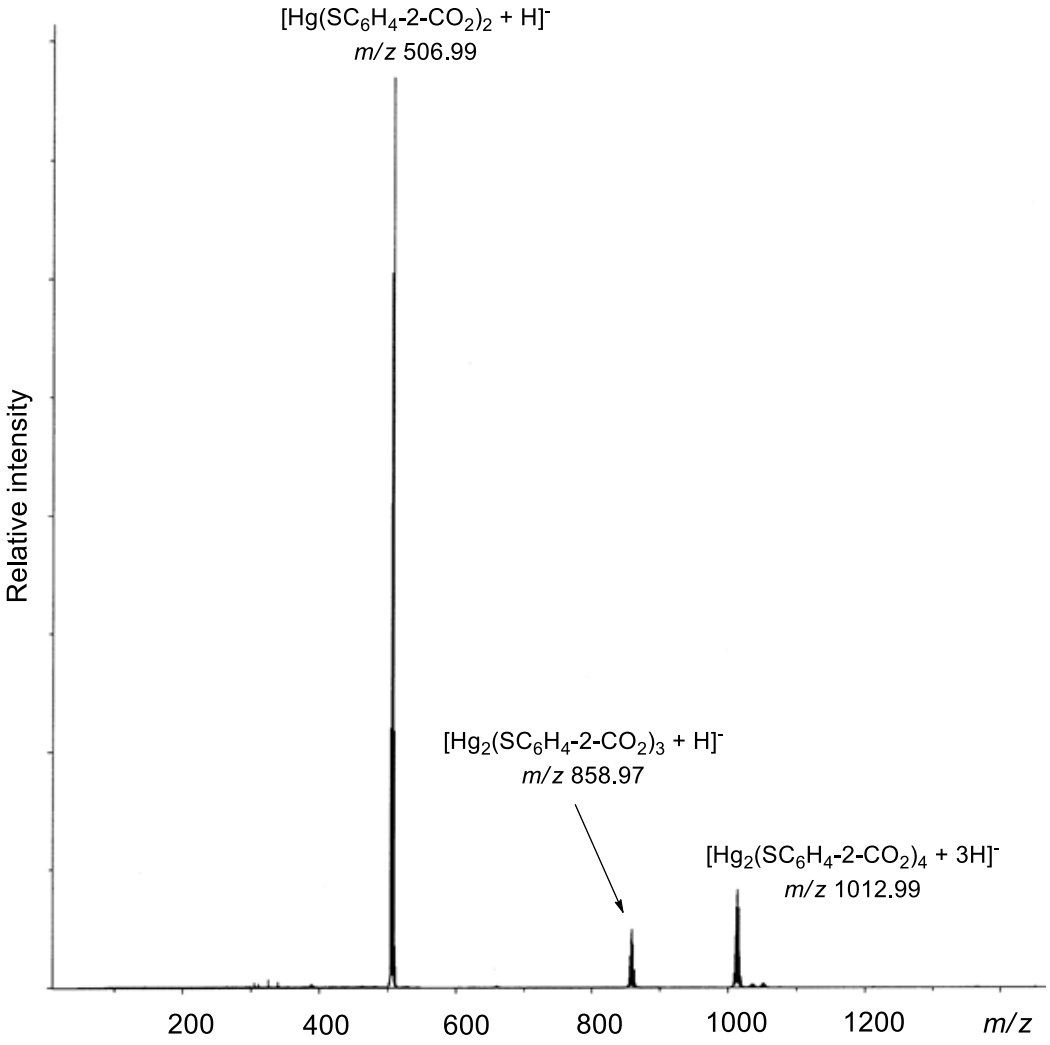

Fig. 3 Negative-ion ESI mass spectrum of **5** in pyridine-methanol solution at a capillary exit voltage of 120 V.

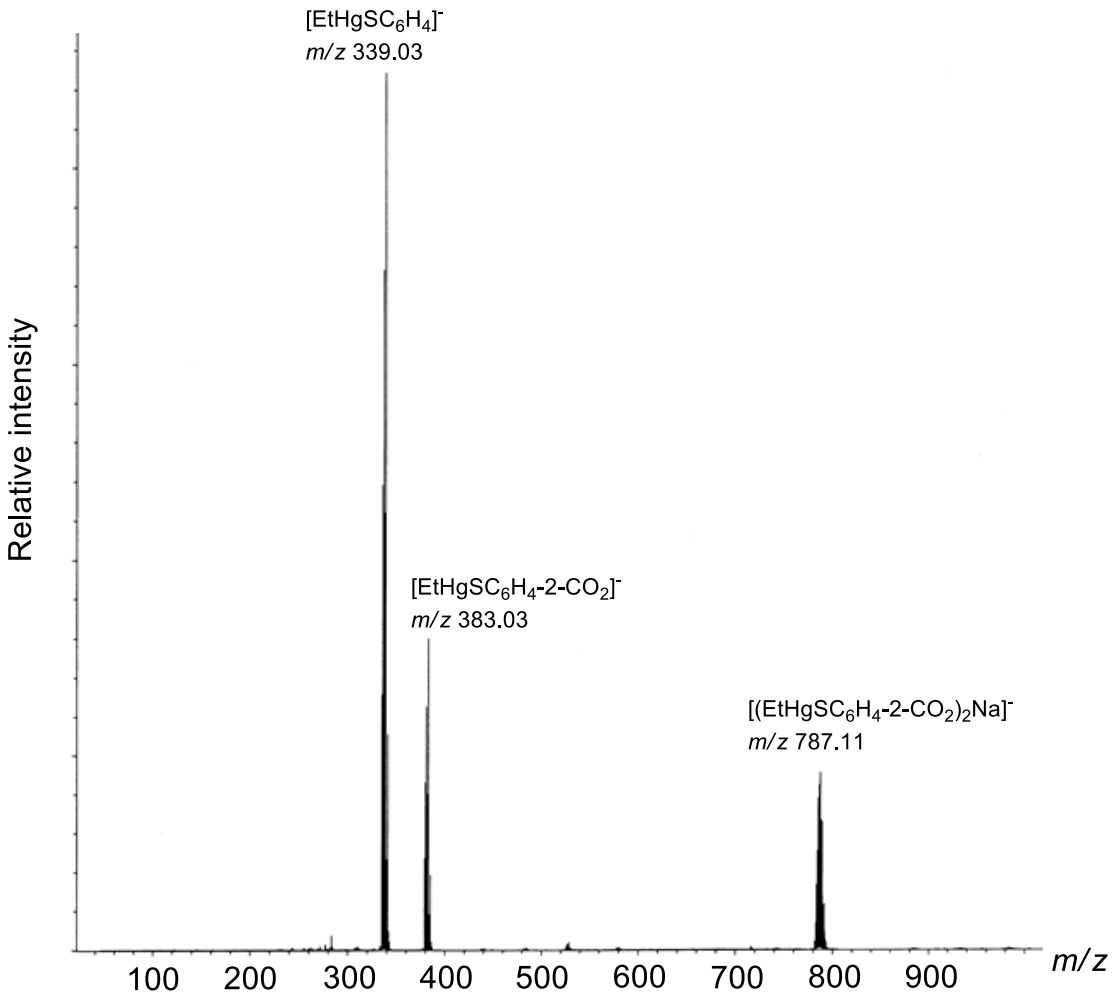

Fig. 4 Negative-ion ESI mass spectrum of *Thiomersal* Na[$EtHgSC_6H_4$-2-CO_2] in methanol at a capillary exit voltage of 150 V.

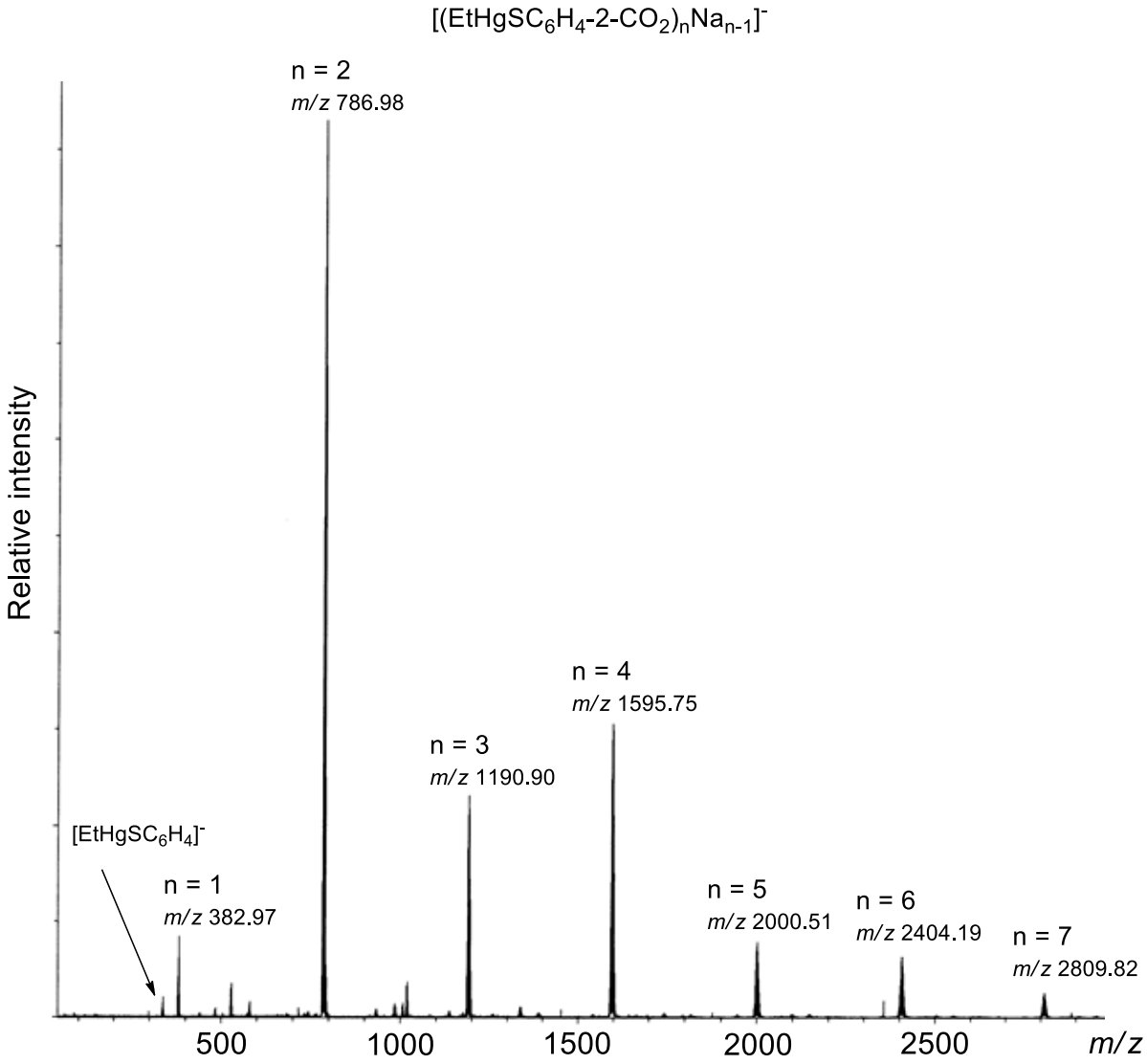

Fig. 5 Wide range negative-ion ESI mass spectrum of *Thiomersal* Na[$EtHgSC_6H_4$-2-CO_2] in methanol at a capillary exit voltage of 150 V showing the formation of aggregate ions [$(EtHgSC_6H_4$-2-$CO_2)_nNa_{n-1}]^-$.

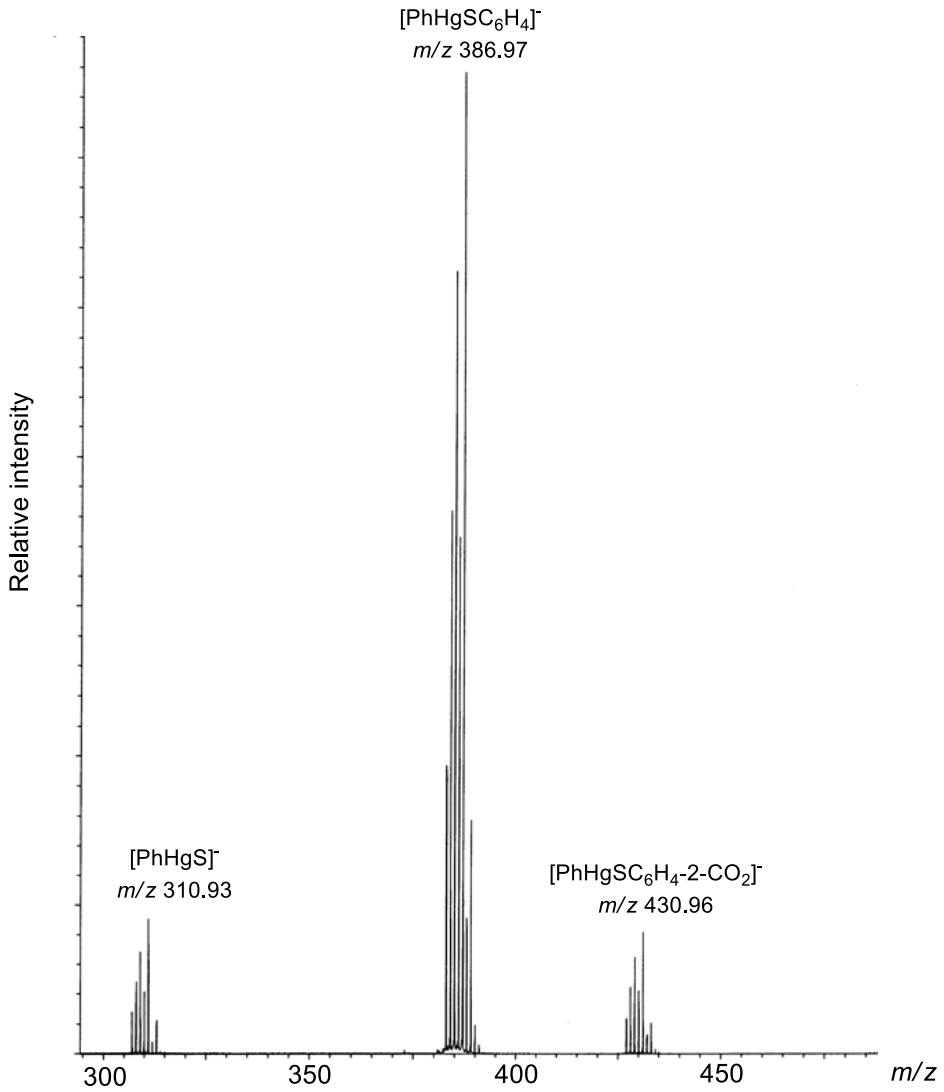

Fig. 6 Negative ion ESI mass spectrum of Na[$PhHgSC_6H_4$-2-CO_2] in methanol at a capillary exit voltage of 150 V showing the formation of fragment ions [$PhHgSC_6H_4$]$^-$ and [PhHgS]$^-$.

References

[1] T. Wehr-Candler, W. Henderson, Coord. Chem. Rev. 313 (2016) 111.

[2] J.S. Roberts in Kirk Othmer Encyclopedia of Chemical Technology, John Wiley & Sons, Inc. (2000) http://dx.doi.org/10.1002/0471238961.2008091518150205.a01

[3] P. Cardiano, D. Cucinotta, C. Foti, O. Giuffrè, S. Sammartano, J. Chem. Eng. Data 56 (2011) 1995.

[4] G. Sachs, H. Blessl, Berichte 58B (1925) 1493.

[5] N.S. Al-Niaimi, B.M. Al-Saadi, J. Inorg. Nucl. Chem. 36 (1974) 1617.

[6] G. Rabbani, A.A. Isab, A.R. Al-Arfaj, S. Ahmad, M. Saleem, A. Hameed, E. Akbar, Spectroscopy 23 (2009) 45.

[7] B.M. Alsaadi, M. Sandstrom, Acta Chem. Scand. A36 (1982) 509.

[8] D.A. Geier, L.K. Sykes, M.R. Geier, J. Toxicol. Env. Health, Part B 10 (2007) 575.

[9] W. Sattler, K. Yurkerwich, G. Parkin, Dalton Trans. (2009) 4327.

[10] M.K. Khoul, Curr. Sci. 45 (1976) 295.

[11] M.K. Khoul, Curr. Sci. 44 (1975) 426.

[12] B.M. Al Saadi, Acta Chem. Scand. A36 (1982) 137.

[13] M.K. Koul, K.P. Dubey, J. Inorg. Nucl. Chem. 35 (1973) 2567.

[14] W. Henderson, B.K. Nicholson, Inorg. Chim. Acta 357 (2004) 2231.

[15] E.R.T. Tiekink, Coord. Chem. Rev. 345 (2017) 209.

[16] E.R.T. Tiekink, W. Henderson, Coord. Chem. Rev. 341 (2017) 19.

[17] C.R. Groom, I.J. Bruno, M.P. Lightfoot, S.C. Ward, Acta Crystallogr. Sect. B 72 (2016) 171.

[18] J. Li-Kao, O. González, R.F. Baggio, M.T. Garland, D. Carrillo, Acta Crystallogr. Sect. C 51 (1995) 575.

[19] L.J. McCaffrey, W. Henderson, B.K. Nicholson, J.E. Mackay, M.B. Dinger, *J. Chem. Soc., Dalton Trans.*, 1997, 2577.

[20] M.B. Dinger, W. Henderson, J. Organomet. Chem. 560 (1998) 233.

[21] R. Janzen, M. Schwarzer, M. Sperling, M. Vogel, T. Schwerdtle, U. Karst, Metallomics 3 (2011) 847.

[22] S. Trümpler, W. Lohmann, B. Meermann, W. Buscher, M. Sperling, U. Karst, Metallomics 1 (2009) 87.

[23] S. Trümpler, B. Meermann, S. Nowak, W. Buscher, U. Karst, M. Sperling, J. Trace Elem. Med. Biol. 28 (2014) 125.

[24] X. Wu, H. Liang, K.A. O'Hara, J.C. Yalowich, B.B. Hasinoff, Chem. Res. Toxicol. 21 (2008) 483.

[25] S. Zhou, M. Hamburger, Rapid Commun. Mass Spectrom. 10 (1996) 797.

[26] N.W. Alcock, P.A. Lampe, P. Moore, J. Chem. Soc., Dalton Trans. (1980) 1471.

[27] J.G. Melnick, G. Parkin, Science 317 (2007) 225.

[28] K.H. Reddy, J. Indian Chem. Soc. 79 (2002) 492.

[29] A.-X. Zheng, H.-X. Li, K.-P. Hou, J. Shi, H.-F. Wang, Z.-G. Ren, J.-P. Lang, Dalton Trans. 41 (2012) 2699.

[30] T. Kaneko, H. Takeuchi, Y. Minoru, Y. Ide, JP 35007599 B 19600621 (1960).

[31] J.H. Waldo, H.S. Shonle, H.M. Powell, J. Bacteriol. 21 (1931) 323.

[32] J.H. Waldo, J. Am. Chem. Soc. 53 (1931) 992.

[33] M. Döring, G. Hahn, M. Stoll, A. C. Wolski, Organometallics, 16 (1997) 1879.

[34] R.W. Kondrat, G.A. McClusky, R.G. Cooks, Anal. Chem. 50 (1978) 1222.

[35] G.A. McClusky, R.W. Kondrat, R.G. Cooks, J. Am. Chem. Soc. 100 (1978) 6045.

[36] R.A.J. O'Hair, N.J. Rijs, Acc. Chem. Res. 48 (2015) 329.

[37] A.P. Jacob, P.F. James, R.A.J. O'Hair, Int. J. Mass Spectrom. 255-256 (2006) 45.

[38] H. Lavanant, E. Hecquet, Y. Hoppilliard, Int. J. Mass Spectrom. 185/186/187 (1999) 11 and references therein.

[39] M.J. Deery, T. Fernandez, O.W. Howarth, K.R. Jennings, J. Chem. Soc., Dalton Trans. (1998) 2177.

[40] M. Strohalm, M. Hassman, B. Košata, M. Kodíček, Rapid Commun. Mass Spectrom. 22 (2008) 905.

[41] R.W. Fish, M. Rosenblum, J. Org. Chem. 30 (1965) 1253.

[42] H.O. House, V.K. Jones, G.A. Frank, J. Org. Chem. 29 (1964) 3327; L. Horner and A. Mentrup, Ann. 65 (1961) 646.

[43] Agilent Technologies, CrysAlisPro, Santa Clara, CA, USA, 2013.

[44] G.M. Sheldrick, Acta Crystallogr. Sect. A 64 (2008) 112.

[45] G.M. Sheldrick, Acta Crystallogr. Sect. C 71 (2015) 3.

[46] L.J. Farrugia, J. Appl. Crystallogr. 45 (2012) 849.

[47] J. Gans, D. Shalloway, J. Mol. Graph. Model. 19 (2001) 557.

[48] DIAMOND, Visual Crystal Structure Information System, Version 3.1, Crystal Impact, Postfach 1251, D-53002 Bonn, Germany, 2006.

[49] A.L. Spek, Acta Crystallogr. Sect. D 65 (2009) 148.